

# Supernova light-curve fitters and Dark Energy

Gabriel R. Bengochea<sup>1,\*</sup>

<sup>1</sup>*Instituto de Astronomía y Física del Espacio (IAFE),  
CC 67, Suc. 28, 1428 Buenos Aires, Argentina*

We show that when a procedure is made to remove the tension between a supernova Ia (SN Ia) data set and observations from BAO and CMB, there might be the case where the same SN Ia set built with two different light-curve fitters behaves as two separate and distinct supernova sets, and the tension found by some authors between supernova sets actually could be due to tension or inconsistency between fitters. We also show that the information of the fitter used in an SN Ia data set could be relevant to determine whether phantom type models are favored or not when such a set is combined with the BAO/CMB joint parameter.

## I. INTRODUCTION

The type Ia supernova (SN Ia) measurements remain a key ingredient in all current determinations of cosmological parameters. More than a decade ago, combined observations of nearby and distant SNe Ia led to the discovery of the accelerating universe picture. It has become clear that different cosmological observations, such as the dimming of distant SNe Ia [1–3], anisotropies in the cosmic microwave background (CMB) [4], and the signature of baryon acoustic oscillation (BAO) [5, 6] cannot be explained with a cosmological model that contains only baryonic and dark matter according to a FRW standard model. The most popular solution is to introduce an extra component with negative pressure, the so-called dark energy (e.g., [7–11]).

Characterization of dark energy focuses on estimation of the equation of state  $w$ , which is the ratio of pressure to density. For the time-invariant  $w = -1$ , the equation of state is consistent with a cosmological constant. Any other fixed or time variable value of  $w$  would require more exotic models.

It is a known fact that the same SN Ia data set in which distance estimates are analyzed with two different light-curve fitters, the values achieved for various cosmological parameters (for example, the equation of state of dark energy) differ, or also there could be found that some cosmological models result more favored than others (e.g. [12–17]).

Here we analyze the consistency between the fitters MLCS2k2 [18] (hereafter MLCS) and SALT2 [19] from a particular approach as it will be further explained. The Multicolor Light Curve Shape fitter, MLCS, is the most recent incarnation of the fitter used by the High-z Supernova Team [2], whilst the Spectral Adaptive Light curve Template, SALT2, is an improved version of the fitter used originally by the Supernova Cosmology Project [1]. A detailed description of both fitters and a thorough discussion about systematic errors in SN surveys can be found for example in [12, 13].

Each method results in a distance modulus for each supernova. However, distance moduli calculated for the same objects by the two fitting methods are not necessarily equal. Whereas the MLCS calibration uses a nearby training set of SNe Ia assuming a close to linear Hubble law, SALT2 uses the whole data set to calibrate empirical light curve parameters. SNe Ia from beyond the range in which the Hubble law is linear are used, so a cosmological model must be assumed in this method. Typically a  $\Lambda$ CDM or a  $w$ CDM ( $w = \text{const}$ ) model is assumed. Consequently the published values of SN Ia distance moduli obtained with SALT2 fitter retain a degree of model dependence. Regarding this, in [20] it was pointed out that systematic errors in the method of SNe Ia distance estimation have come into sharper focus as a limiting factor in SN cosmology. The major systematic concerns for supernova distance measurements are errors in correcting for host-galaxy extinction and uncertainties in the intrinsic colors of supernovae, luminosity evolution, and selection bias in the low-redshift sample. Also, SALT2 fitter does not provide a cosmology-independent distance estimate for each supernova, since some parameters in the calibration process are determined in a simultaneous fit with cosmological parameters to the Hubble diagram.

In [21] it was investigated the tension between SN Ia data sets (Constitution [12] and Union [22]) and other data sets, CMB and BAO. There, it was shown that SN Ia data sets are in tension not only with the observations of CMB and BAO, but also with other SN Ia data sets such as Davis07 [23]. It was also shown that in the Davis07 data set there is no tension with CMB and BAO observations, concluding that Union and Constitution data sets are in tension not only with the observations of CMB and BAO, but also with other SN Ia data sets. Then, the author found the main sources responsible for the tension by employing a truncation method, following the simple procedure used in [24]. With this in mind, the truncated UnionT and ConstitutionT data sets were built, which are consistent with the other observations and the tension was completely removed.

In the quest of the characterization of dark energy, in [25] it was first noted that observational data do not rule out the possibility that  $w < -1$ . Phantom dark energy models with  $w < -1$  have the interesting properties that

---

\*Electronic address: gabriel@iafe.uba.ar

the density of the dark energy increases with increasing scale factor, and the phantom energy density can become infinite at a finite time, a condition known as the ‘big rip’.

Future projects as SNAP [26] are designed to reveal the nature of the dark energy. It will characterize the dark energy density, equation of state and time variation by precisely and accurately measuring the distance-redshift relation of SNe Ia. The matter density, dark energy density, and flatness of the universe could be determined at the 1% level, including systematic uncertainties, the dark energy equation of state to about 3% and its time variation characterized to within 10% of the Hubble expansion time. In summary, this kind of project will seek to determine whether  $w = -1$  or not, and if  $w$  is a constant or it evolves in time. However, in order to do this, the matter of reducing the systematic uncertainties between light-curve fitters will be of great importance. The combination of observational data sets might lead, as it will be further shown, the equation of state of dark energy to be of the phantom type or not, depending on how the SN Ia data were processed.

In this Letter we focus on the consistency of two of the main light-curve fitters used for the elaboration of SN Ia data sets. To accomplish this, we present another approach to the tension between SN Ia data sets as the one found in [21] and then the consistency between light-curve fitters is analyzed when appears the need of removing tension between an SN Ia data set and BAO/CMB data applying a truncation method to the same SN Ia data set, but obtained with the two different fitters. Additionally, we show that the conclusion about if the combination of SN Ia data with BAO/CMB favors or not an equation of state for dark energy of the phantom type in the framework of a given cosmological model might depend, in some cases, on the fitter employed in the elaboration of the SN Ia set used in the analysis.

## II. TENSION BETWEEN SUPERNOVAE IA DATA SETS REVISITED

In this section and the next one we will use a  $\chi^2 = \chi_{SNe}^2 + \chi_{BAO/CMB}^2$  statistic to analyze the confidence intervals of the free parameters of two cosmological models, by employing different SN Ia data sets and their combination with the BAO/CMB joint parameter introduced in [14]. Since lately more non-standard models are built to try to explain the dark energy phenomenon, we chose to combine the SNe analysis with the BAO/CMB joint parameter which is better suited for these sort of models, using it only as an example of data combination. We must also clarify that the goal of this work was neither to put constraints nor to find best fits to cosmological models, but to show certain extra information that should be minded when non-SNe data sets are combined with SNe data sets analyzed with different fitters. The separate  $\chi^2$  of SNe Ia and BAO/CMB used in this work are shown in Appendix A.

We considered for the analysis the  $\Lambda$ CDM and flat  $w$ CDM models with  $w = const$ . In the case of  $\Lambda$ CDM the dark energy is a cosmological constant which behaves as a vacuum energy with  $w = -1$ , but we allowed non-zero spatial curvature  $\Omega_k$ . Then the dimensionless expansion rate is given by,

$$E \equiv H(z)/H_0 = [\Omega_m(1+z)^3 + \Omega_r(1+z)^4 + \Omega_k(1+z)^2 + \Omega_\Lambda]^{1/2} \quad (1)$$

where  $H(z)$  is the Hubble parameter as a function of the cosmological redshift  $z$ ;  $\Omega_m$ ,  $\Omega_r$  and  $\Omega_\Lambda$  are the contributions of matter, radiation and dark energy respectively to the total energy density today, and the curvature density is  $\Omega_k = 1 - \Omega_m - \Omega_r - \Omega_\Lambda$ . The parameters usually chosen as free parameters in this model are  $\Omega_m$  and  $\Omega_\Lambda$ .

For the flat  $w$ CDM ( $\Omega_k = 0$ ) case, we allowed the equation of state parameter of dark energy  $w$  to differ from -1 so,

$$E = [\Omega_m(1+z)^3 + \Omega_r(1+z)^4 + \Omega_\Lambda(1+z)^{3(1+w)}]^{1/2} \quad (2)$$

where now  $\Omega_\Lambda = 1 - \Omega_m - \Omega_r$ . The free parameters in this model are  $\Omega_m$  and  $w$ . The case flat  $\Lambda$ CDM is a special case of this one.

The choice of the considered models for this analysis was arbitrary and not relevant, this was for mere simplicity (two free parameters) with the aim of showing the novel results. The consideration of models with an equation of state  $w$  that does not evolve in time is enough, since the current data do not yield precise constraints on the time derivative of  $w$ . (For constraints on time-varying  $w$ , see [14] as an example). Additionally, the rationale for the flat case of  $w$ CDM was that the WMAP data from the CMB anisotropy constrain the spatial curvature to be very small (e.g. [27]). Also, the use of these two models is the most suitable to obtain a correct comparison among different fitters, since the light-curve fitter SALT2 uses the whole data set to calibrate empirical light curve parameters and a  $\Lambda$ CDM or a  $w$ CDM model is typically assumed, as it was mentioned in Section I.

As it was previously mentioned, the analysis in this work was performed in the framework of SALT2 [19] and MLCS [18] fitters and the SN Ia data sets used were Constitution data sets (Tables 2 and 4 from [12] as it will be further explained in Section III), the SDSSII full data set (Tables 10 and 14 from [13] with the same values used for the ‘intrinsic’ dispersions there) and the Union2 data set [3].

It was interesting to observe the discrepancy between the results obtained when using one fitter or the other when it is allowed the variation of  $\Omega_k$  in the framework of a  $\Lambda$ CDM ( $w = -1$ ) model. The analysis of the SDSSII full data set with 288 SNe Ia built with MLCS showed that the flat case ( $\Omega_m = 0.27$  [4]) stands excluded to more than  $3\sigma$  confidence level, while with the same data set, but processed with SALT2 this did not happen at all (Figs. 1a and 1c). Something similar happens in the framework of the flat  $w$ CDM model (Figs. 1b and 1d):

the standard model ( $\Omega_m = 0.27, w = -1$ ) using SDSSII (MLCS) is excluded to more than  $2\sigma$  confidence level (see also Fig.1 of [14]). Since the responsible of this fact is the fitter and not the SNe Ia (because the data set is the very same and only the fitter was changed), one could then wonder what SN Ia data set should be used to be combined with, for example CMB data, which leave little margin to the variation of  $\Omega_k$  (e.g. [27]). Looking at Figs. 1c and 1d one would choose those data sets processed with SALT2; however we should keep in mind that SALT2 fitter retains a degree of model dependence because typically a  $\Lambda$ CDM model is assumed.

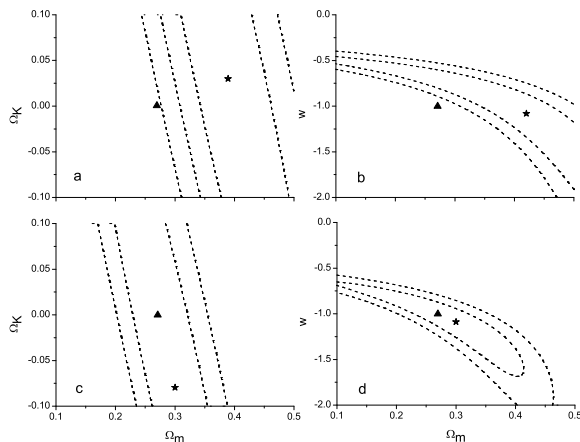


FIG. 1: (a) Confidence intervals at 68.3%, 95.4% and 99.7% in the  $\Omega_m - \Omega_k$  plane for the SDSSII (MLCS) SN Ia data set in the  $\Lambda$ CDM model framework (dashed lines). (b) Confidence intervals at 68.3% and 95.4% in the  $\Omega_m - w$  plane for the SDSSII (MLCS) SN Ia data set in the flat  $w$ CDM model framework (dashed lines). (c) Confidence intervals at 68.3% and 95.4% in the  $\Omega_m - \Omega_k$  plane for the SDSSII (SALT2) SN Ia data set in the  $\Lambda$ CDM model framework (dashed lines). (d) Confidence intervals at 68.3% and 95.4% in the  $\Omega_m - w$  plane for the SDSSII (SALT2) SN Ia data set in the flat  $w$ CDM model framework (dashed lines). The best fits are indicated with a star whereas the standard flat  $\Lambda$ CDM ( $\Omega_m = 0.27$ ) is marked with a triangle.

In [21], it was found that Union [22] and Constitution [12] data sets were in tension not only with BAO and CMB data, but with other SN Ia data sets too (e.g. Davis07 [23]). The tension found was attributed to certain supernovae of the data set and by a truncation method these outliers were removed from the set with the objective of releasing the tension.

We found interesting to analyze what would happen if we applied a criterion in order to study the consistency between data sets, a criterion more restrictive than the only fact that the confidence intervals overlap. To perform this analysis, we adopted the criterion of considering the existence of tension between a given data set and

another set constituted combining several data sets (including the first one) as the fact that the best fit point to the first data set is out of the 68.3% ( $1\sigma$ ) confidence level contour given by the combined data set. Similar criteria were adopted in their analysis by [21, 24, 28, 29]. This is a criterion we will adopt in order to show how differently will behave the same SN Ia set processed with two different fitters when a truncation method is performed. This will lead to an alternative way of analyzing the discrepancy between the results obtained when one or other fitter is used. One could choose not to use this more restrictive criterion, nevertheless with this adopted criterion, we seek more physical consistency between best-fits, so the best fits do not drive to too different cosmological evolutions. A best fit which effective equation of state is of the phantom type [25] ( $w < -1$ ) tells us about very different physics from the one that is not. For instance, in a recent work [29] the consequences of applying it to several data sets in the framework of  $f(T)$  theories have been investigated.

When we used the Union2 recently released data set with 557 SNe Ia (processed with SALT2 fitter) to combine it with the information from BAO/CMB in the framework of the flat  $w$ CDM model, we found that there is no tension between data sets (Fig. 2a). However, when we did the same procedure with the 288 SNe Ia of the SDSSII set (in the framework of MLCS fitter) we found that there is tension between SNe Ia and BAO/CMB to more than  $3\sigma$  (Fig. 2b). Since the data from BAO/CMB are the same used in both cases, one could wrongly conclude that there is tension between the SN Ia data sets. This case is similar to what was found in [21]. The result

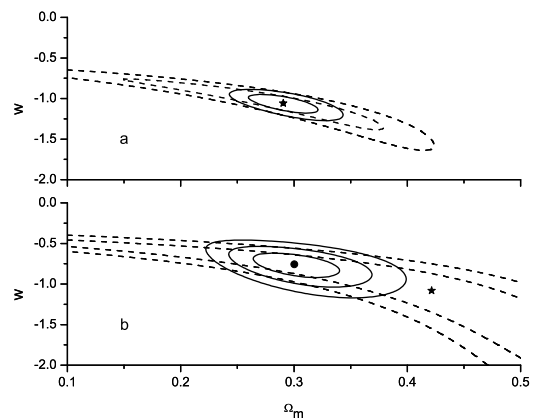


FIG. 2: (a) Confidence intervals at 68.3% and 95.4% in the  $\Omega_m - w$  plane for the Union2 (SALT2) SNe Ia only (dashed lines) and Union2+BAO/CMB (solid lines). (b) Confidence intervals at 68.3%, 95.4% and 99.7% in the  $\Omega_m - w$  plane for the SDSSII (MLCS) SNe Ia only (dashed lines) and SDSSII+BAO/CMB (solid lines). The best fits to SNe are indicated with a star whereas the best fits to the combined parameters are indicated with a dot.

obtained in [21], where there is tension between Union and BAO, while in Davis07 there is none, seems to be due to a data set (Union) is processed with SALT and the other (Davis07) with versions of MLCS. The tension between Union and Davis07 could actually be a trouble between fitters and not between supernovae sets as it will be discussed in the next section.

To better understand the analysis of tension between Union2 and SDSSII performed here, in Figs. 3a and 3b are displayed the combinations of SNe Ia+BAO/CMB for the Union2 and SDSSII cases respectively. For the case Union2 vs SDSSII(MLCS) there is tension to more than  $2\sigma$  level, while in Union2 vs SDSSII(SALT2) there is none. Clearly the tension exists between fitters and not between SN Ia data sets.

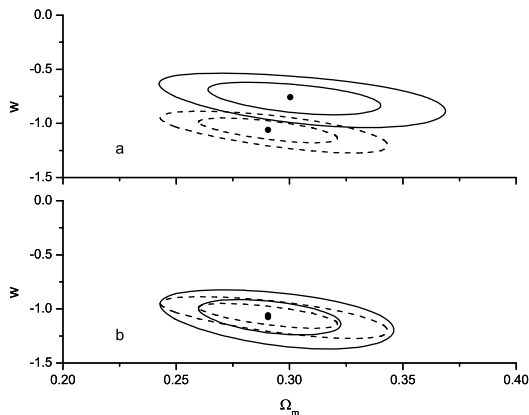


FIG. 3: Confidence intervals at 68.3% and 95.4% in the  $\Omega_m - w$  plane from combining SNe Ia+BAO/CMB. (a) Union2 (SALT2 - dashed lines) vs SDSSII (MLCS - solid lines). (b) Union2 (SALT2 - dashed lines) vs SDSSII (SALT2 - solid lines). A tension between fitters is revealed.

### III. ARE SUPERNOVAE LIGHT-CURVE FITTERS CONSISTENT?

In this section we analyze the problem of tension between light-curve fitters and the consistency between them from a different approach.

We found interesting to study what happens when one needs to perform a truncation procedure as in [21] to remove the tension between BAO/CMB and an SN Ia data set (processed with a given fitter) and the same SN Ia data set but with a different fitter. It is important to emphasize that the adopted criterion itself is not relevant, but how the same SN set behaves when it is processed with different fitters.

The criterion consists in finding and removing the outliers responsible of the tension. First, we fitted the model to the whole SN Ia data set finding the best fit parameters, including the nuisance parameter  $\mu_0$  (see Appendix

A). Then, we calculated the relative deviation to the best fit prediction,  $|\mu_{obs} - \mu_{th}| / \sigma_{obs}$ , for all the data points finding which cut solved the tension problem and which SNe Ia were the outliers.

We performed this procedure in the framework of the flat  $w$ CDM model for two different SN Ia data sets, Constitution (SALT2 and MLCS) and SDSSII (SALT2 and MLCS).

For the data sets here denominated Constitution (SALT2) and Constitution (MLCS) we used the same 337 SNe Ia from the Table 2 (SALT2) and Table 4 (MLCS17) from [12]. In [12] MLCS was used to find the dust-reddening properties through the value of  $R_V$  that minimizes the scatter in the Hubble residuals for the nearby CfA3 sample and they found  $R_V = 1.7$ . MLCS with  $R_V = 3.1$  overestimates host-galaxy extinction while  $R_V = 1.7$  does not. With its lower value of  $R_V$ , MLCS17 attributes less host extinction to each SN Ia and therefore this produces a larger distance compared to MLCS31.

Figure 4a shows the confidence intervals to 68.3% and 95.4% in the plane  $\Omega_m - w$  for the Constitution (SALT2) data set of SNe Ia only and for the combination SNe Ia+BAO/CMB. There, a tension to  $2\sigma$  confidence level between both data sets can be observed. In Fig. 4b it is shown that after the truncation procedure with a  $2.1\sigma$  cut (13 outliers) the tension was removed completely. In a similar way, we proceeded to do the same with the Constitution (MLCS) data set and the results are shown in Figs. 5a and 5b. In this case, a  $2\sigma$  cut was enough and 12 SNe Ia were removed from the data set so the tension with BAO/CMB was removed. Although the necessary cut for Constitution set was slightly different for SALT2 than for MLCS, and although the number of SNe to remove was not significantly different, the most remarkable fact was that *only 4 outliers were the same*. This can be clearly seen in Table I where SNe Ia outliers are displayed for each case and which of those are the ones in common. We want to stress that the SN Ia data set was the same and the only difference lied in the light-curve fitter employed. Then, with this truncation procedure we found *the behavior was as if there were two different SN Ia sets when actually there was only one*.

Something more drastic occurred when we did the same analysis, but using the SDSSII data set. When the SDSSII (SALT2) data set was used, no SNe Ia needed to be removed, since there was no tension with BAO/CMB (Fig. 6a). However, with the SDSSII (MLCS) data set there was tension with BAO/CMB to a level greater than 99.7% (Fig. 6b) and a cut of  $1.7\sigma$  (18 outliers) was needed to remove such tension. To highlight this, in Fig. 7 we show the confidence intervals to 99.7% of the combined SNe Ia+BAO/CMB for the cases SDSSII (SALT2) and SDSSII (MLCS). There, it can be seen how both best fits differ by more than  $3\sigma$  level. Another interesting thing is the comparison of Figs 7 and 3a. This comparison allows appreciating how *two light-curve fitters employed for the same SN Ia set produce the same result than two different SN Ia sets*.

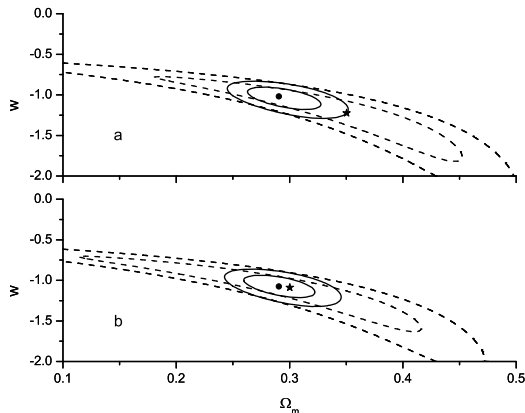


FIG. 4: (a) Confidence intervals at 68.3% and 95.4% in the  $\Omega_m - w$  plane for the Constitution (SALT2) SNe Ia only (dashed lines) and SNe+BAO/CMB (solid lines). Tension can be appreciated between data sets. (b) Idem (a), but after performing the truncation procedure. The best fits to SNe are indicated with a star whereas the best fits to the combined parameters are indicated with a dot.

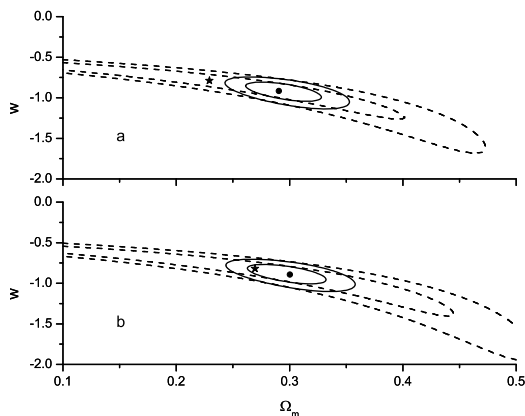


FIG. 5: (a) Confidence intervals at 68.3% and 95.4% in the  $\Omega_m - w$  plane for the Constitution (MLCS) SNe Ia only (dashed lines) and SNe+BAO/CMB (solid lines). Tension can be appreciated between data sets. (b) Idem (a), but after performing the truncation procedure. The best fits to SNe are indicated with a star whereas the best fits to the combined parameters are indicated with a dot.

The fact of needing to take out different supernovae to remove the tension in Constitution (SALT2) and in Constitution (MLCS) reveals that they are not the supernovae themselves that probably generate the tension, but the fitters. Using the same SN Ia data set with the same truncation process, the SNe Ia we had to take out were not the same ones. It seems as if a given fitter makes some supernovae bring an apparent problem. The case

TABLE I: The outliers after the truncation procedure by using the same Constitution SN Ia data set processed with MLCS and SALT2 light-curve fitters. Note that there are only 4 matches in the outlier SNe.

Constitution	
MLCS	SALT2
04D3dd	04D3cp
	04D3oe
	d033
d083	d083
	d084
	e138
f221	f221
isis	isis
k430	
	mceenroe
	sn00ce
sn02hd	
	sn05ir
sn06cg	
sn07bz	sn07bz
sn07ci	
sn92br	
sn97dg	
sn98ab	
	vilas

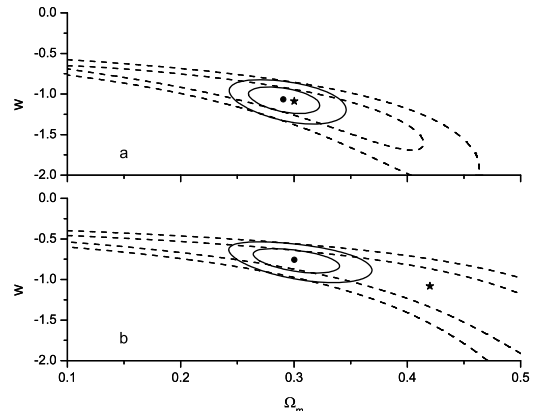


FIG. 6: (a) Confidence intervals at 68.3% and 95.4% in the  $\Omega_m - w$  plane for the SDSSII (SALT2) SNe Ia only (dashed lines) and SNe+BAO/CMB (solid lines). There is no tension between the data sets. (b) Idem (a), but for the SDSSII (MLCS) SNe Ia. Here can be appreciated tension to more than  $2\sigma$  confidence level.

of the SDSS data set also presented this behavior, because with one fitter there were supernovae that caused tension and with the other there were none, since there was no need of truncation. What we found here with two different fitters for the same SN Ia data set is analogue to what was found in [21] between two different SN Ia sets. What was found between Union and Davis07 data sets is perhaps a fitter problem and not supernovae.

We also analyzed another interesting aspect. We found important to stress how an employed fitter in an SN Ia data set could take part in the conclusion about the

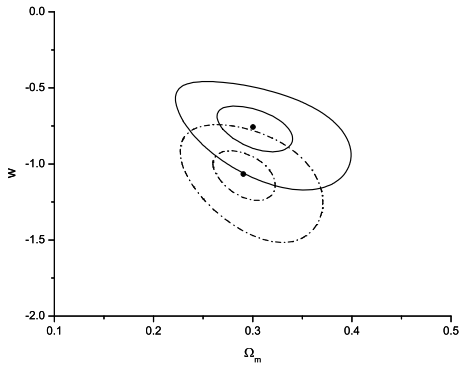


FIG. 7: Confidence intervals at 68.3% and 99.7% in the  $\Omega_m - w$  plane coming from combining SN Ia and BAO/CMB data. Solid lines correspond to SDSSII (SALT2) whereas dash-dotted lines correspond to SDSSII (MLCS). There can be seen that both best fits are outside  $3\sigma$  confidence level from the other fitter.

equation of state  $w$  of a given model when this SN Ia set is combined with BAO/CMB, being this joint parameter more suitable for the lately more common non-standard models. In Table II (Phantom Table) we show how for two given theories using the combination BAO/CMB+SN Ia (SALT2) is obtained a best fit for  $w$  of the phantom type, while with MLCS the opposite occurs. There, the result is shown for the flat  $w$ CDM model and for a non-standard model of modified gravity  $f(T)$  as in [29, 30] when Union2 (SALT2), SDSSII (SALT2 and MLCS) and Constitution (SALT2 and MLCS) are used.

TABLE II: *Phantom Table*. Best fit  $w$  types for two cosmological models when the BAO/CMB joint parameter is combined with an SN Ia data set processed with a given light-curve fitter.

Model	BAO/CMB +	Best fit $w$ type
Flat $w$ CDM	Union2 (SALT2)	Phantom
Flat $w$ CDM	SDSSII (SALT2)	Phantom
Flat $w$ CDM	SDSSII (MLCS)	non-Phantom
Flat $w$ CDM	Const.(SALT2)	Phantom
Flat $w$ CDM	Const.(MLCS)	non-Phantom
$f(T)$	Union2 (SALT2)	Phantom
$f(T)$	SDSSII (SALT2)	Phantom
$f(T)$	SDSSII (MLCS)	non-Phantom
$f(T)$	Const.(SALT2)	Phantom
$f(T)$	Const.(MLCS)	non-Phantom

We do not mean that this is going to occur with any model, but to conclude that the combination of data sets favors or not phantom type models with  $w < -1$ , the fitter used to process the SNe Ia is an additional factor that must be taken into account as source of degeneration.

## IV. CONCLUSIONS

Although the evidence in the FRW framework that the universe is going through an accelerated stage, because of the existence of what we call dark energy, is solid from various observational data sets, its nature will depend on the future better understanding of the systematic errors present in supernovae observations, particularly those present in the light-curve fitters analyzed here.

As it is well known, when the same SN Ia data set is processed with two different fitters, the values found for cosmological parameters (such as the equation of state of dark energy) differ.

Here we analyzed this difference showing how when a procedure to remove tension between an SN Ia data set and observations from BAO/CMB is performed, there could exist the case where the same SN Ia set processed with two different fitters behaves as if there were two different sets, and the tension between sets found by some authors actually could be due to a tension or inconsistency between fitters.

We also showed that the information of the fitter used in an SN Ia set could be relevant and it should be minded as an additional factor to decide if phantom type models are favored or not when the given SN Ia set is combined with the BAO/CMB joint parameter.

## Acknowledgments

G.R.B. is supported by CONICET. I would like to thank Tamara Davis and Jesper Sollerman for kind and helpful discussions about SDSS SNe Ia data sets. Also, I thank Diego Travieso for his numerical collaboration and interesting discussions and Rafael Ferraro for his support.

## Appendix A: Cosmological constraints methods

### 1. Type Ia Supernovae constraints

The  $N$  data points of the SNe Ia compiled in a data set are usually given in terms of the distance modulus  $\mu_{obs}(z_i)$ . On the other hand, the theoretical distance modulus is defined as

$$\mu_{th}(z_i) = 5 \log_{10} D_L(z_i) + \mu_0 \quad (A1)$$

where  $\mu_0 \equiv 42.38 - 5 \log_{10} h$  and  $h$  is the Hubble constant  $H_0$  in units of 100 km/s/Mpc, whereas the Hubble-free luminosity distance for the general case is,

$$D_L(z) = (1+z) |\Omega_k|^{-1/2} \mathcal{S}_k \left[ |\Omega_k|^{1/2} \int_0^z \frac{dz'}{E(z', \mathbf{p})} \right] \quad (A2)$$

in which  $E \equiv H(z)/H_0$  is the dimensionless expansion rate,  $\mathbf{p}$  denotes the model parameters, and the function

$\mathcal{S}_k(x) = \sin(x)$  when the curvature density  $\Omega_k < 0$ ,  $\mathcal{S}_k(x) = \sinh(x)$  for  $\Omega_k > 0$  and  $\mathcal{S}_k(x) = x$  for the flat case  $\Omega_k = 0$ . Correspondingly, the  $\chi^2$  from the N SNe Ia is given by

$$\chi_{SNe}^2(\mathbf{p}) = \sum_{i=1}^N \frac{[\mu_{obs}(z_i) - \mu_{th}(z_i; \mathbf{p})]^2}{\sigma^2(z_i)} \quad (\text{A3})$$

where  $\sigma(z_i)$  is the corresponding uncertainty for each observed value. The parameter  $\mu_0$  is a nuisance parameter but it is independent of the data points. One can perform a uniform marginalization over  $\mu_0$ . However, there is an alternative way. Following [31], the minimization with respect to  $\mu_0$  can be made by expanding the  $\chi_{SNe}^2$  of (A3) with respect to  $\mu_0$  as

$$\chi_{SNe}^2(\mathbf{p}) = \tilde{A} - 2\mu_0\tilde{B} + \mu_0^2\tilde{C} \quad (\text{A4})$$

where,

$$\begin{aligned} \tilde{A}(\mathbf{p}) &= \sum_{i=1}^N \frac{[\mu_{obs}(z_i) - \mu_{th}(z_i; \mu_0 = 0, \mathbf{p})]^2}{\sigma^2(z_i)} \\ \tilde{B}(\mathbf{p}) &= \sum_{i=1}^N \frac{[\mu_{obs}(z_i) - \mu_{th}(z_i; \mu_0 = 0, \mathbf{p})]}{\sigma^2(z_i)} \\ \tilde{C} &= \sum_{i=1}^N \frac{1}{\sigma^2(z_i)} \end{aligned}$$

Eq. (A4) has a minimum for  $\mu_0 = \tilde{B}/\tilde{C}$  at

$$\tilde{\chi}_{SNe}^2(\mathbf{p}) = \tilde{A}(\mathbf{p}) - \frac{\tilde{B}(\mathbf{p})^2}{\tilde{C}} \quad (\text{A5})$$

Since  $\chi_{SNe, min}^2 = \tilde{\chi}_{SNe, min}^2$  obviously, we can instead minimize  $\tilde{\chi}_{SNe}^2$  which is independent of  $\mu_0$ .

## 2. Combined BAO/CMB parameter constraints

Since in this work we combined CMB and BAO observations with SN Ia data sets for flat models, we consider here all the relations for the spatially flat case.

A more model-independent constraint can be achieved by multiplying the BAO measurement of  $r_s(z_d)/D_V(z)$  with the position of the first CMB power spectrum peak [27]  $\ell_A = \pi d_A(z_*)/r_s(z_*)$ , thus canceling some of the dependence on the sound horizon scale [14]. Here,  $d_A(z_*)$  is the comoving angular-diameter distance to recombination,  $r_s$  is the comoving sound horizon at photon decoupling,  $z_d \approx 1020$  is the redshift of the drag epoch at

which the acoustic oscillations are frozen in, and  $D_V$  is defined as (assumed a  $\Lambda$ CDM model) [5],

$$D_V(z) = \left[ \frac{z}{H(z)} \left( \int_0^z \frac{dz'}{H(z')} \right)^2 \right]^{1/3} \quad (\text{A6})$$

We further assume  $z_* = 1090$  from [27] (variations within the uncertainties about this value do not give significant differences in the results).

In [6] was measured  $r_s(z_d)/D_V(z)$  at two redshifts,  $z = 0.2$  and  $z = 0.35$ , finding  $r_s(z_d)/D_V(0.2) = 0.1905 \pm 0.0061$  and  $r_s(z_d)/D_V(0.35) = 0.1097 \pm 0.0036$ . Combining this with  $\ell_A$  gives the combined BAO/CMB constraints [14]:

$$\begin{aligned} \frac{d_A(z_*)}{D_V(0.2)} \frac{r_s(z_d)}{r_s(z_*)} &= 18.32 \pm 0.59 \\ \frac{d_A(z_*)}{D_V(0.35)} \frac{r_s(z_d)}{r_s(z_*)} &= 10.55 \pm 0.35 \end{aligned} \quad (\text{A7})$$

Before matching to cosmological models we also need to implement the correction for the difference between the sound horizon at the end of the drag epoch and the sound horizon at last scattering. The first is relevant for the BAO, the second for the CMB, and  $r_s(z_d)/r_s(z_*) = 1.044 \pm 0.019$  (using values from [27]). Inserting this into (A7) and taking into account the correlation between these measurements using the correlation coefficient of 0.337 calculated by [6], gives the final constraints we use for the cosmology analysis [14]:

$$\begin{aligned} A_1 &= \frac{d_A(z_*)}{D_V(0.2)} = 17.55 \pm 0.65 \\ A_2 &= \frac{d_A(z_*)}{D_V(0.35)} = 10.10 \pm 0.38 \end{aligned} \quad (\text{A8})$$

Using this BAO/CMB parameter cancels out some of the dependence on the sound horizon size at last scattering. This thereby removes the dependence on much of the complex pre-recombination physics that is needed to determine that horizon scale [14]. In all the cases, we have considered a radiation component  $\Omega_r = 5 \times 10^{-5}$ .

So, for our analysis we add to the  $\chi^2$  statistic:

$$\chi_{BAO/CMB}^2(\mathbf{p}) = \sum_{i=1}^{N=2} \frac{[A_{obs}(z_i) - A_{th}(z_i; \mathbf{p})]^2}{\sigma_A^2(z_i)} \quad (\text{A9})$$

where  $\mathbf{p}$  are the free parameters,  $A_{obs}$  is the observed value ( $A_1$  and  $A_2$ ),  $A_{th}$  is the predicted value by the model and  $\sigma_A$  is the  $1\sigma$  error of each measurement.

[1] Perlmutter S. et al., Bull. Am. Astron. Soc. **29**, (1997) 1351; Astrophys. J. **517**, (1999) 565;

[2] Riess A. G. et al., Astron. J. **116**, (1998) 1009; Astron. J. **607** (2004) 665.

- [3] Amanullah R. et al., *Astrophys. J.* **716**, (2010) 712.
- [4] Komatsu E. et al., *Seven-year Wilkinson Microwave Anisotropy Probe (WMAP) observations: cosmological interpretation*, arXiv:1001.4538.
- [5] Eisenstein D. et al., *Astrophys. J.* **633**, (2005) 560.
- [6] Percival W. J. et al., *MNRAS* **401**, (2010) 2148.
- [7] Huterer D. and Turner M. S., *Phys. Rev.* **D60**, (1999) 081301.
- [8] Sahni V. and Starobinsky A. A., *Int. J. Mod. Phys.* **D9**, (2000) 373.
- [9] Padmanabhan T., *Phys. Rep.* **380**, (2003) 235.
- [10] Frieman J., Turner M. S. and Huterer D., *Annu. Rev. Astron. Astrophys.* **46**, (2008) 385.
- [11] Huterer D., *The Accelerating Universe*, arXiv:1010.1162.
- [12] Hicken M. et al., *Astrophys. J.* **700**, (2009) 1097.
- [13] Kessler R. et al., *Astrophys. J. Suppl. Ser.* **185**, (2009) 32.
- [14] Sollerman J. et al., *Astrophys. J.* **703**, (2009) 1374.
- [15] Bueno Sanchez J. C. et al., *Comparison of recent  $S_nIa$  datasets*, arXiv:0908.2636.
- [16] Pigozzo C. et al., *Background test for  $\Lambda(t)CDM$  cosmology*, arXiv:1007.5290.
- [17] Smale P. R. and Wiltshire D. L., *Supernova tests of timescape cosmology*, arXiv:1009.5855.
- [18] Phillips M. M. et al., *Astrophys. J.* **413**, (1993) L105; Riess A. G. et al., *Astrophys. J.* **438**, (1995) L17; Jha S. et al., *Astrophys. J.* **659**, (2007) 122.
- [19] Guy J. et al., *Astron. and Astrophys.* **466**, (2007) 11.
- [20] Frieman J. A., *AIP Conf. Proc.* **1057**, (2008) 87.
- [21] Wei H., *Phys. Lett.* **B687**, (2010) 286.
- [22] Kowalski M. et al., *Astrophys. J.* **686**, (2008) 749.
- [23] Davis T. M. et al., *Astrophys. J.* **666**, (2007) 716.
- [24] Nesseris S. and Perivolaropoulos L., *JCAP* **0702**, (2007) 025.
- [25] Caldwell R. R., *Phys. Lett.* **B545**, (2002) 23.
- [26] <http://snap.lbl.gov>.
- [27] Komatsu E. et al., *Astrophys. J. Suppl.* **180**, (2009) 330.
- [28] Li M. et al., *Revisit of tension in recent  $S_nIa$  datasets*, arXiv:0910.0717.
- [29] Bengochea G. R., *Observational information for  $f(T)$  theories and Dark Torsion*, *Phys. Lett.* **B** (2010), doi:10.1016/j.physletb.2010.11.064, arXiv:1008.3188.
- [30] Bengochea G. R. and Ferraro R., *Phys. Rev.* **D79**, (2009) 124019.
- [31] Nesseris S. and Perivolaropoulos L., *Phys. Rev.* **D72**, (2005) 123519; Perivolaropoulos L., *Phys. Rev.* **D71**, (2005) 063503.